Estimation of the Digitized Mammographic Breast Density by the Histogram Approach Using the Neural Network

Sachiko Goto[1)], Yoshiharu Azuma[2)], Tetsuhiro Sumimoto[3)], Yoshihiro Takeda[4)] and Shigeru Eiho*

Faculty of Health Sciences, Okayama University Medical School
Fax: +81-86-222-3717
1) Email: goto@md.okayama-u.ac.jp
2) Email: azuma@md.okayama-u.ac.jp
3) Email: sumimoto@md.okayama-u.ac.jp
4) Email: ytakeda@md.okayama-u.ac.jp
*Graduate School of Informatics, Kyoto University
Fax: +81-774-38-3938, Email: eiho@image.kuass.kyoto-u.ac.jp

Abstract – Our aim was to improve the accuracy of classifying x-ray mammographic breast densities. The histogram approach using the neural network was used for the purpose of constructing a flexible system. In this study the phantom of the synthetic breast-equivalent resin material for the process of the A/D conversion of mammograms was employed. The digital values can offset the difference in characteristics between the mammography system, the unit, etc. Furthermore the features of our system use the neural network, and then tune the neural network by the histogram of the digital values and by the radiologists' and expert mammographers' assessment ability. Although there was an observer's bias, our system was able to classify the breast density automatically according to that observer. This is only possible if the observer has been trained to some extent and is capable of maintaining an objective assessment according to the assessment criteria.

Keywords – breast density, classification, histogram.

I. Introduction

Information derived from x-ray mammographic breast densities (breast densities) provides one of the strongest indicators of the risk of breast cancer [1]. In clinical practice, radiologists routinely estimate the breast density of mammograms by using the BI-RADS lexicon as recommended by the American College of Radiology [2]. Since their evaluation is performed visually, many studies of objective class division employ the process of the A/D conversion of x-ray mammograms, digital image processing, and the extraction of a characteristic value. However, since the digital value changes depending on the characteristics of the mammography system, the x-ray film and the digitizer, research results were variable. In this study we employed the phantom of the synthetic breast-equivalent resin material (breast-equivalent phantom) for the process of the A/D conversion of the mammograms, as both a physical and general method. That is, we adopted the breast model thatconsisted of the uniform mixture of adipose and glandular tissue. It can be assumed that a breast component consists of adipose and glandular tissue in

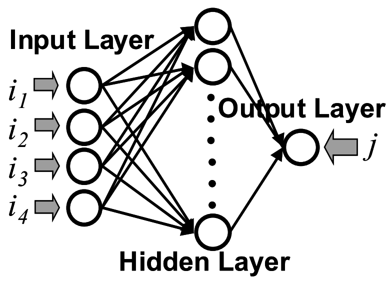

Data Set		
i_1	Tube Voltage (26-31 kV)	
i_2	mAs (10-120 mAs)	
i_3	Thickness of breast-equivalent phantom (2-6 cm)	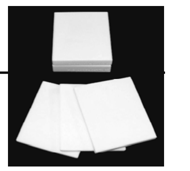
i_4	Glandular rate of breast-equivalent phantom (0-100%)	
j	Pixel Value of digital-image of breast-equivalent phantom (0-65535)	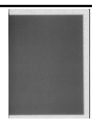

Figure 1. Structure of the back-propagation neural network (BPNN-1) for producing the converting curves of digital values to glandular rates.

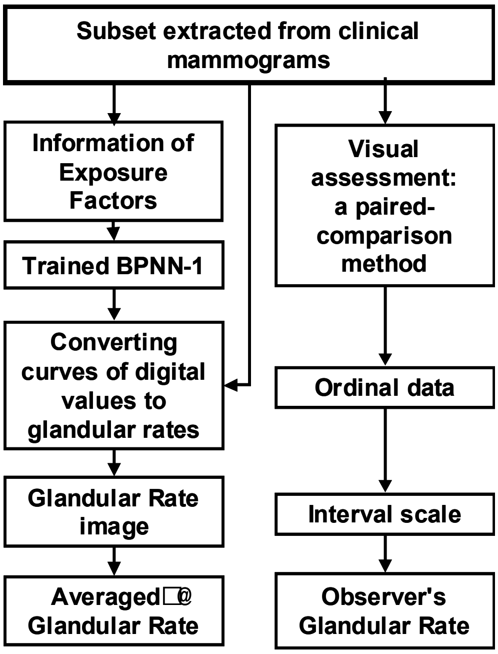

Figure 2 The process of calculation by the trained BNPP-1and visual assessment of Glandular Rate.

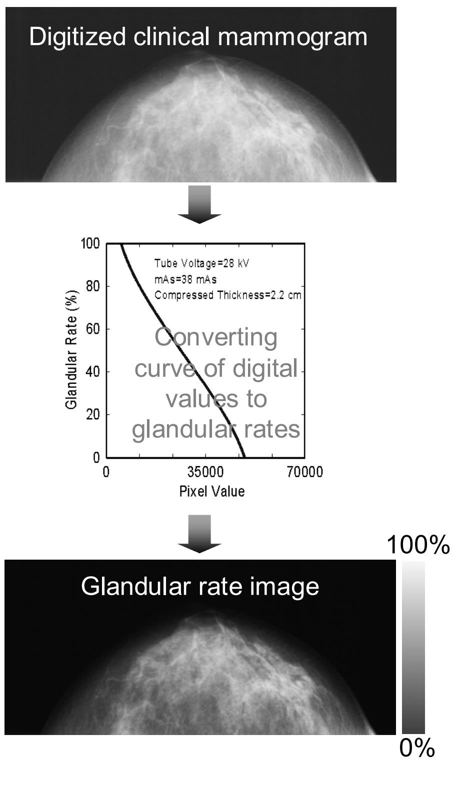

Figure 3 Conversion to glandular rate image of digitized clinical mammogram.

attenuation coefficients of x-rays for adipose and glandular tissue. These tissues produce the breast densities. Pixel values of digitized mammograms were converted to glandular rates by the trained neural network with the digitized breast-equivalent phantom images of known glandular rate. Furthermore the glandular rate images were classified into the BI-RADS categories with the histogram approach using the neural network that was trained by radiologists' and expert mammographers' assessment ability.

II. MATERIALS AND METHODS

First, the back-propagation neural network-1 (BPNN-1) was trained by the dataset, which consisted of the exposure factors of a number of breast tissue equivalent phantoms of varying thickness and glandular rates, and of the average pixel value of the digitized breast tissue equivalent phantom image of known glandular rate, as shown in Figure 1. Next, 100 samples from clinical mammograms were prepared as the subset, from which x-ray generator data and compressed breast thickness had been recorded. The glandular rates of the subset were computed in the process shown on the left-hand side of Figure 2. When the data of the subset was input into the trained BPNN-1, the curve (converting curve of digital values to glandular rates) was used to convert a digitized mammogram to a glandular rate image as shown in Figure 3. An average glandular rate was computed by pixel values within the breast area. On the other hand, the subjective visual assessment by radiologists and expert mammographers was performed on the subset in the process shown on the right-hand side of Figure 2. The method of analysis of paired comparisons based on the Thurstone-Mosteller model [3] was used to perform ranking of breast density of the subset and to transform rank ordinal data to interval scale. The three radiologists and 4 expert mammographers performed the visual assessment in each class. After the interval scales were connected through classes 1-4, the glandular-occupation rates (%) were given to the maximum and minimum interval scales by the radiologists and then the glandular-occupation rates of all the samples were calculated.

An adaptive dynamic range compression technique [4] was applied to the glandular rate image to reduce the range of the glandular rates' level of distribution in the low frequency background and to enhance the differences in the characteristic features of the glandular rate histogram. The glandular rate histogram within the breast area was generated and normalized, and passed through an averaging window to smooth out the random fluctuations. In each histogram for each glandular image, a glandular rate threshold corresponding to the glandular-occupation rate was investigated by visual assessment and was named as the visual threshold. Furthermore, the minimum glandular rate, average glandular rate, glandular rate of each main peak, maximum frequency value and the energy (E) ratio of the lower region to the higher region were also investigated as characteristic values of the histograms. In order to further lessen the deviation between BPNN-1 and the visual assessment, one more back-propagation neural network (BPNN-2) was prepared as shown in Figure 4. In training the BPNN-2, the classified results and visually-assessed thresholds were set as output data, and four-histogram characteristic values were input into the BPNN-2. The round-robin (i.e. leave-one-out) method was used to test the generalization ability of the total system (Figure 5) for this data set.

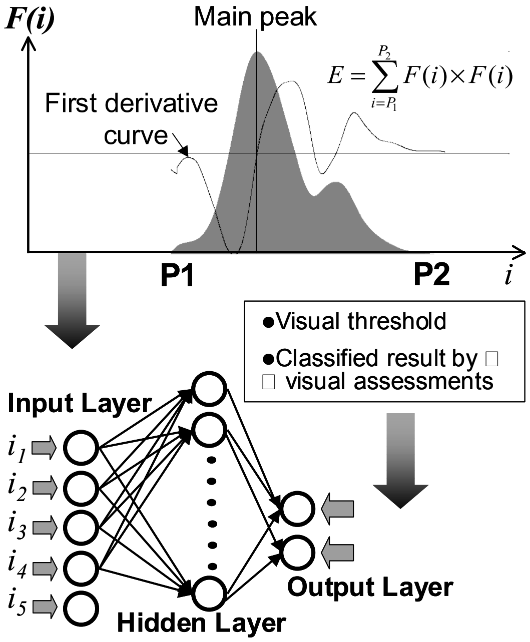

Figure 4 Structure of the back-propagation neural network (BPNN-2) for classification and glandular rate.

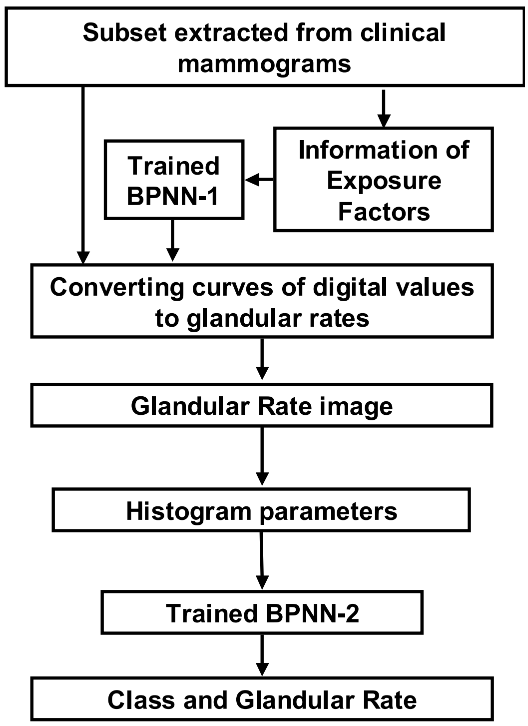

Figure 5 The calculation process of the classification and glandular rate by BPNN-1 and BPNN-2.

III. Results and Discussion

The gray circles in Figure 6 show the comparison between the visual assessment results and the calculation results by BPNN-1 in the glandular rate for the subset. The glandular rate became higher as the difference between visual estimation and calculated result increased. The circles in Figure 6 show the comparison between the visual assessment results and the calculation results by BPNN-1 and BPNN-2 in the glandular-occupation rate for 30 samples in the subset after the performance test by the round-robin method. The residual sum of squares shows that the accuracy of the calculation result by BPNN-1 and BPNN-2 increased. The difference in the distribution shows that the values of the calculated results improved as the glandular rate became higher. The table shows the performance of BNPP-1 and -2.

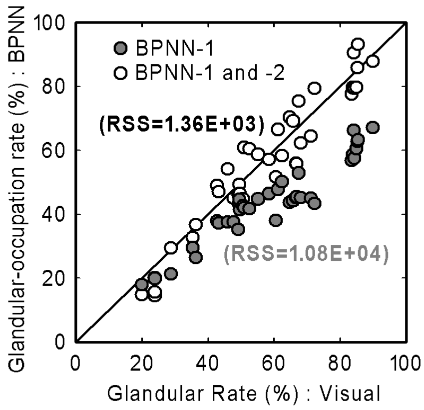

Figure 6 The comparison between the visual assessment results and the calculation results by BPNN-1 and BPNN-1 and -2 in the glandular rate for Subset-B. The value in a parenthesis is the residual sum of squares.

Table
Performance Of The BPNN-1 And BNPP-1 And-2 In Each Class

	Sensitivity (%)	Specificity (%)
Class 1	100	100
Class 2	88.9	96.6
Class 3	87.5	95.6
Class 4	100	96.7

$$\text{Sensitivity} = \frac{\text{True positive fraction}}{\text{True positive fraction} + \text{False negative fraction}}$$

$$\text{Specificity} = \frac{\text{True negative fraction}}{\text{False positive fraction} + \text{True negative fraction}}$$

The glandular rates after BPNN-1 with the breast-equivalent phantom are not dependent on the characteristics of the mammography system, the x-ray film or the digitizer. Thus, we consider that the processing using the glandular rates is general. Although there is some observer bias, our system can calculate a reliable value close to that observer's, providing they are trained to some extent and are capable of balancing their criteria of assessment against their internal variation. However, when pure physical analysis of a mammogram is required, an observer's bias can create error; for example, in the estimation of the glandular rate for the calculation of the patient dose etc. In that case, if BPNN-1 only is used as shown in Figure 2, our system can also respond to such a situation.

IV. CONCLUSION

For the general classification of breast densities of x-ray mammograms into four classes in the BI-RADS, the A/D conversion of mammograms with the breast-equivalent phantom and the neural network were used. Then the neural network was tuned by radiologists' and expert mammographers' assessment ability. Our system is not only capable of classifying the breast density of mammograms but can also provide qualitative analysis.

REFERENCES

[1] J. N. Wolfe, "Breast Patterns as index of risk for developing cancer", Am. J. Roentgenol., 126, 1130-1139, 1976.

[2] American College of Radiology, Breast imaging reporting and Data system (BI-RADS), 3rd Ed, 1998.

[3] L. L. Thurstone, "The method of paired comparisons for social values", Journal of Abnormal and Social Psychology, 1927b 21, 384-400, 1927.

[4] Chuan Zhou, Heaning-Ping Chan. Nicholas Petrick, et al., "Computerized image analysis: Estimation of breast density on mammograms", Med. Phys., 23, June, 2001.